EARTH SCIENCES
RESEARCH JOURNAL
Earth Sci. Res. J. Vol. 28, No. 2 (June, 2024): 213 - 229

UNIVERSIDAD NACIONAL DE COLOMBIA

METEOROLOGY

Climatic temperature indices for the coastal resilience observatory in Tabasco (Dos Bocas)–LANRESC

Mercedes Andrade-Velázquez[1]*, Martín José Montero-Martínez[2], M. F. Vargas Magaña[3]
1. CONAHCYT–Centro del Cambio Global y la Sustentabilidad (CCGS). Villahermosa, Tabasco, México. mercedes.andrade@ccgs.mx
2. Instituto Mexicano de Tecnología del Agua. Subcoordinación de Eventos Extremos y Cambio Climático, Jiutepec, Morelos. martin_montero@tlaloc.imta.mx
3. División de Ciencias Básicas, Universidad Juárez Autónoma de Tabasco, Cunduacán, Tabasco, México. fernandavargasmagana@gmail.com
*Corresponding author: mercedes.andrade@ccgs.mx

ABSTRACT:

This study focused on calculating climate change indices derived from maximum and minimum temperature variables for the Coastal Resilience Observatory in Tabasco, Dos Bocas, located in Paraíso, Tabasco, Mexico. The indices were computed using CLIMPACT2, 2007 version, and a total of 26 indices were obtained for the period from 1940 to 2022. Subsequently, significant trends were calculated using statistical tests such as Mann-Kendall, trend-free prewhitening, bias correction applied to prewhitening, and variance correction (by two methods). Sen's slope method was employed to determine the extent of alteration in extreme climate indices. Increasing trends were found in the indices tn90p (%), tx90p (%), tr (days), txgt50p (%), wdsi (days), su (days), tmge10 (days), tmge5 (days), gddgrow (days), and gsl (days), indicating the presence of local warming and providing evidence of climate change detection. These results contribute to updating climate information in the area and serve as a proposal for replication in the other six Coastal Observatories of the National Coastal Resilience Laboratory in Mexico, as part of measures related to climate stressors in coastal areas where these observatories are located. This information is valuable for decision-makers and the general population, as it will support socio-environmental adaptation and mitigation measures in the face of climate change as part of efforts to enhance the resilience of socioecosystems in coastal areas.

Keywords: climate change; temperature indices; coastal zone; Tabasco-Mexico.

Índices climáticos de temperatura para el observatorio de resiliencia costera en Tabasco (Dos Bocas)–LANRESC

RESUMEN:

El presente trabajo se centró en el cálculo de índices de cambio climático derivados de las variables de temperatura máxima y mínima para el Observatorio Costero de Resiliencia en Tabasco, Dos Bocas, ubicado en el municipio de Paraíso, Tabasco, México. Los índices fueron calculados mediante CLIMPACT2, versión 2007, y se obtuvieron un total de 26 para el período de 1940-2022. Posteriormente, se calcularon las tendencias significativas mediante pruebas estadísticas de Mann-Kendall, preblanqueamiento sin tendencia, corrección de sesgo aplicada al preblanqueamiento, corrección de varianza (por dos vías), y se utilizó la pendiente de Sen como método para determinar el grado de alteración de los índices climáticos extremos. Se encontraron tendencias de aumento en los índices de tn90p (%), tx90p (%), tr (días), txgt50p (%), wdsi (días), su (días), tmge10 (días), tmge5 (días), gddgrow (días) y gsl (días), mostrando así que existe calentamiento local y evidenciando la detección del cambio climático. Estos resultados contribuyen a la actualización de información climática en la zona y representan una propuesta para ser replicada en los otros seis observatorios costeros del Laboratorio Nacional de Resiliencia Costera en México, como parte de las medidas relacionadas con los estresores climáticos en las zonas costeras donde se ubican dichos observatorios. Esta información es útil para los tomadores de decisiones y la población en general, ya que permitirá respaldar medidas de adaptación y mitigación sociambientales ante el cambio climático, como parte de las acciones hacia una mejor resiliencia de los socioecosistemas en las zonas costeras.

Palabras clave: cambio climático; índices de temperatura; zonas costeras; Tabasco-México.

Record
Manuscript received: 02/01/2024
Accepted for publication: 30/07/2024

How to cite this article:
Andrade-Velázquez, M. A., Montero-Martínez, M. J., & Vargas-Magaña, M. F. (2024). Climatic temperature indices for the coastal resilience observatory in Tabasco (Dos Bocas)–LANRESC. *Earth Sciences Research Journal, 28*(2), 213-229. https://doi.org/10.15446/esrj.v28n2.112335

1. Introduction

The phenomenon of Climate Change is unequivocal and has been described in the Assessment Report 5 (AR5) of the Intergovernmental Panel on Climate Change (IPCC) as "a change in the state of the climate that can be identified (e.g., using statistical tests) by changes in the mean and/or the variability of its properties, and that persists for an extended period, typically decades or longer. Climate change may be due to natural internal processes or external forcings." The United Nations Framework Convention on Climate Change (UNFCCC), in its Article 1, defines climate change as: "a change of climate which is attributed directly or indirectly to human activity that alters the composition of the global atmosphere and which is in addition to natural climate variability observed over comparable time periods*"*. Currently, climate change is evident on a global scale. The Intergovernmental Panel on Climate Change (IPCC) highlighted in its 2007 report the expected changes in weather patterns due to global warming, including an increase in the frequency and intensity of extreme weather events. The report mentioned above is a special document dedicated to the study of changes in extreme events in the context of climate change. Coastal areas are among the most vulnerable communities to climate change (IPCC, 2022). Therefore, the ability to measure climate change on variables such as temperature and precipitation is crucial to enable these communities to adapt adequately to possible impacts. By using climate indicators, communities can anticipate and adapt to changes, thus minimizing the risks associated with climate change. Tabasco has highly vulnerable coastal areas throughout Mexico, primarily due to its geographical location, extensive plain, and susceptibility to flooding due to its low elevation (SEMARNAP, 1997; Aparicio et al., 2009; Gama et al., 2010). Historically, it has been affected by severe floods recorded in 1995, 1999, 2007, and more recently in 2020 (CENAPRED, 2021). The floods have varied in magnitude and duration (Arreguín-Cortés et al., 2014). These changes have altered the dynamics of wetlands in coastal areas, which serve the function of "buffering" the threats associated with climate change events (Perevochtchikova & Lezama, 2010; Alizad et al., 2018). These events have affected communities and ecosystems, including the notable effect of coastal erosion, as in the case of Sánchez Magallanes (Hernández-Santana et al., 2008). In Tabasco, approximately 50% of its wetlands have been lost due to illegal logging of mangroves (Hernández Melchor et al., 2017). Anthropogenic activities in coastal areas have left bodies of water contaminated and soil degraded, mainly due to toxic waste that alters the chemical and physical properties of the soil, leading to the death of mangroves (Adams, 1999; García-López et al., 2006; Sandilyan & Kathiresan, 2014; Rastogi et al., 2021). The Tabasqueño landscape has been modified, with approximately 97% of forest resources lost over a period of 50 years (1940 - 1990). This occurred due to excessive forest exploitation, primarily of riparian mangroves and wetlands. This results in dramatic impacts during flood periods, such as increased saline intrusion and coastal erosion (Mata-Zayas et al., 2017).

The National Coastal Resilience Laboratory of Mexico (LANRESC, hereinafter, acronym in Spanish) was founded in 2015 with three partner institutions in Mexico: i) Institute of Engineering, Sisal Unit (UNAM); ii) Sonora Technological Institute (ITSON), and iii) the Center for Global Change and Sustainability (CCGS). Subsequently, additional institutions joined, including the Faculty of Sciences-Sisal Unit, the Faculty of Chemistry-Sisal Unit, the Institute of Economic Research, and the CINVESTAV-Mérida Unit (LANRESC, 2023). In 2018, the establishment of six Coastal Observatories was proposed, and this expanded to seven in 2019, under the name Coastal Observatories for Resilience (OCR, acronym in Spanish), located at seven coastal points in Mexico: three in the Yucatán Peninsula (Sisal, Alacranes Reef, Celestún), one in Oaxaca (Copalita), one in Tabasco (Dos Bocas), one in Campeche (Laguna de Términos), and one in Sonora (Agiabampo). As part of LANRESC's activities through its OCRs, standardized indicators are established in each of them to provide information about the historical and current state of socioecosystems in their various components: environmental, physical, and social. Therefore, the goal is to determine climate indicators in the OCR-Tabasco, as a pilot site, so that they can be extrapolated to the other six OCRs.

It is necessary to pause at this point to define some important concepts commonly used in climate change studies, which will be employed later. These definitions are taken from the AR6 technical report by Working Group II (WGII):

"Vulnerability is a component of risk, but also, independently, an important focus. Vulnerability in this report is defined as the propensity or predisposition to be adversely affected and encompasses a variety of concepts and elements, including sensitivity or susceptibility to harm and lack of capacity to cope and adapt". "Adaptation is defined, in human systems, as the process of adjustment to actual or expected climate and its effects in order to moderate harm or exploit beneficial opportunities. In natural systems, adaptation is the process of adjustment to actual climate and its effects; human intervention may facilitate this". "Resilience is defined as the capacity of social, economic and environmental systems to cope with a hazardous event or trend or disturbance, responding or reorganising in ways that maintain their essential function, identity and structure while also maintaining the capacity for adaptation, learning and transformation".

One way to study recent climate changes and its extremes is through the climate change indices recommended by the now-defunct Expert Team on Climate Change Detection and Indices (ETCCDI) of CCl/WCRP/JCOMM. In the agreements of the 17th edition of the Commission for Climatology of the World Meteorological Organization (WMO, 2018), the ETCCDI was suspended, and the new group responsible for the now Sectoral Climate Indices (SCI) is the Commission on Meteorology, Applications, and Services Related to Climate, Water, and the Environment (SERCOM) -Expert Team on Climate Information for Decision-Making (Montero-Martínez et al., 2022). In Mexico, there are several relatively recent studies that analyzed climate extremes of surface temperature and precipitation using the ETCCDI indices (Montero-Martínez et al., 2018; Pita-Díaz & Ortega-Gaucín, 2020; Colorado-Ruiz & Cavazos, 2021; Montero-Martínez et al., 2022). In the case of surface temperature, where they showed a clear regional warming signal, particularly in the last few decades (Montero-Martínez & Andrade-Velázquez, 2022). The analysis of climatic extremes of surface temperature and precipitation using the ETCCDI indices was carried out by Peterson et al. (2008) for Mexico and by Montero-Martínez et al. (2018) for two basins north and south of Mexico. These indices can provide information on climatic extreme changes over different time periods. For surface temperature, they showed a clear warming signal at the regional level in recent decades (Montero et al., 2022). We note that climatic extremes are determined by the ETCCDI indices and should not be confused with extreme events used in meteorology.

Within the framework and vision of the OCRs of LANRESC, which are strategically located in the coastal zone of Mexico, it is proposed to conduct an analysis of climate indicators at each of the sites. This analysis aims to understand changes in the climatic extremes and to address the climate change on human communities and ecosystems located within or in the vicinity of the OCRs.

2. Study area

The coastal area of Tabasco (Figure 1) is situated between 92° 28' and 94° 10' West longitude and between 17° 5' and 18° 39' North latitude (Hernández-Santana et al., 2008). In Dos Bocas, Paraíso, Tabasco, there is an important industrial and commercial development port for Mexico (SEDEC, 2023). The port is located at a distance of 85 km from the city of Villahermosa, Tabasco (INEGI, 2023). In this port, you can also find the Petroleum Industrial Park, covering an area of 70 ha (SEMAR, 2023). Like the rest of the state, the climate is warm and humid, with an average temperature of 27 °C (INEGI, 2023). Rainfall in the area is due to cold fronts and tropical cyclones in the fall and winter, while in the summer, it is influenced by tropical cyclones and the presence of the Intertropical Convergence Zone, with a dry season mainly in the spring (Andrade-Velázquez, 2017). During this last season, temperatures can reach over 40°C (SMN, 2023). However, changes in extremes of this variable, in past or recent periods in the state, have not been quantified.

3. Materials and methods

The data used is sourced from the ERA5 database (Herbach et al., 2023). It is in a grid format with a resolution of 0.25° x 0.25°. Minimum (TN) and maximum (TX) temperature variables were obtained for the time period from 1940 to 2022 with a daily time window. Climate-relevant indices were calculated based on the region's climatic conditions (see Table 1) using the CLIMPACT2 software, version 2007, designed for Linux (http://fsf.org/).

Initial time conditions were adjusted, including the baseline period, which covered 31 years (1940-1970), and the climate change indices to be computed (Annex A). Once the files for a quadrant covering the southeast of Mexico were obtained, interpolation was carried out using the nearest neighbor method to the point with coordinates latitude 18.434722°, longitude -93.201667°, which corresponds to the location of the municipality of Paraíso, where Dos Bocas is located (see Figure 1). This was done to ensure that the calculation of the indices was not adversely affected.

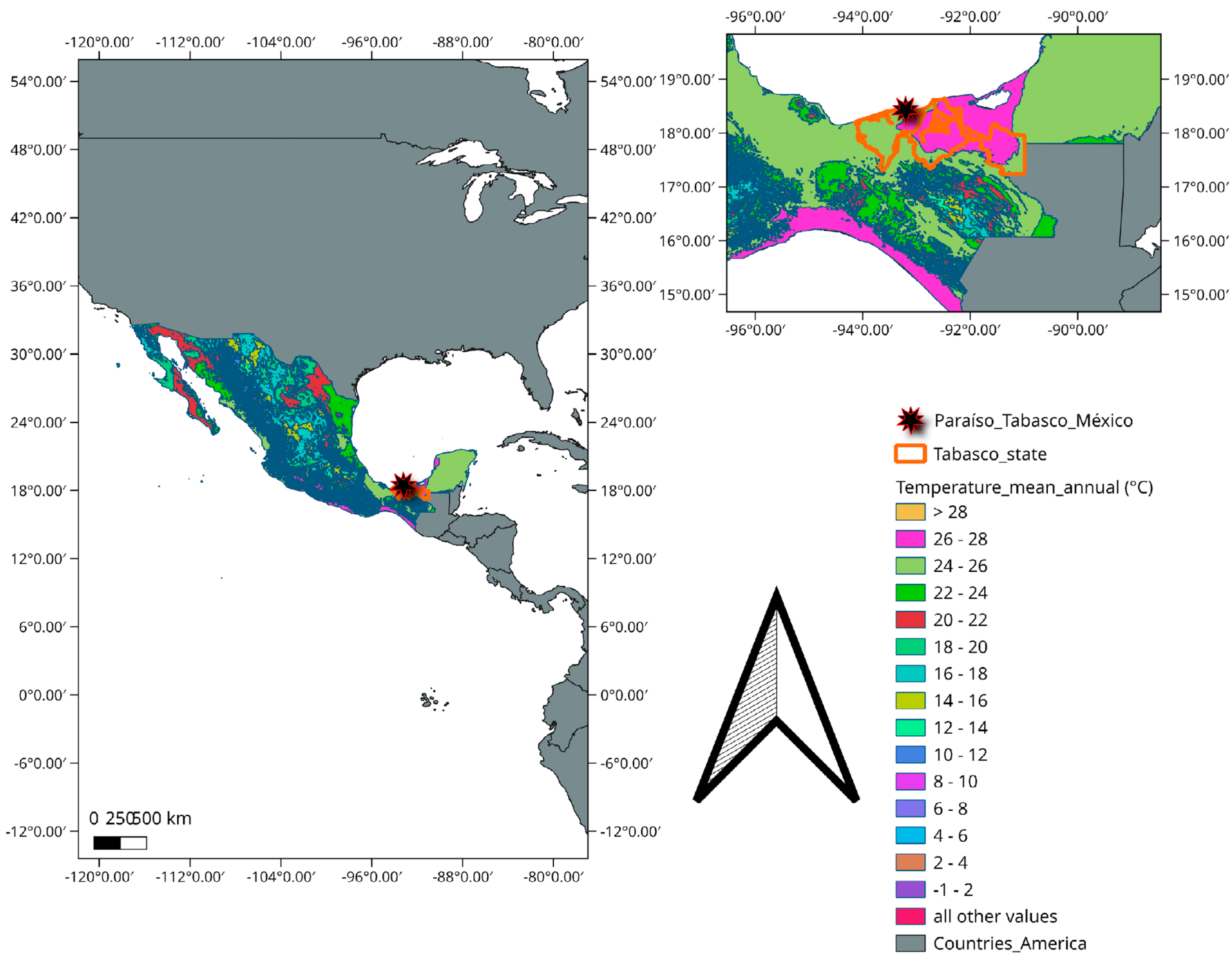

Figure 1. Location of the study area. Dos Bocas, Paraíso, Tabasco, Mexico. The units of the mean annual temperature are °C. Source: CONABIO (2023).

Table 1. Annual climate change indices calculated for the maximum (TX) and the minimum (TN) temperatures. TM means medium temperature, TM = (TX + TN) / 2.

Index	Means	Units
csdi5	Cold spell duration indicator 5-day window (when TN remains below its climatological 10th percentile)	days
csdi	Cold spell duration indicator (when TN remains below its climatological 10th percentile)	days
dtr	Daily Temperature Range	degrees_C
gddgrow10	Growing Degree Days	degree-days
gsl	Growing Season Length	days
hddheat18	Heating Degree Days	degree-days
su	Summer days	days
tmge10	TX of at least 10 degrees_C	days
tmge5	TX of at least 5 degrees_C	days

(Continued)

Index	Means	Units
tmm	Mean TM	degrees_C
tn10p	Amount of cold nights (10th percentile)	%
tn90p	Amount of hot days	%
tnm	Mean TN	degrees_C
tnn	Min TN	degrees_C
tnx	Max TN	degrees_C
tr	Tropical nights	days
tx10p	Amount of cool days	%
tx3tn3	3 consecutive number of hot days and nights	Number of events
tx90p	Amount of hot days	%
txb3tnb3	3 consecutive number of cold days and Nights	Number of events
txge30	TX of at least 30 degrees_C	days
txgt50p	Fraction of days with above average temperature	%
txm	Mean TX	degrees_C
txn	Min TX	degrees_C
txx	Max TX	degrees_C
wsdi5	Warm spell duration indicator (5day)	days
wsdi	Warm spell duration indicator (when the maximum temperature (TX) remains above its climatological 90th percentile)	days

Calculation of trends

A linear fit was applied to each of the indices, following Equation 1:

$$y = mx + b \tag{1}$$

Where m represents the slope, which determines the trend, b is the y-intercept, x is the independent variable (in this case, time), and y is the dependent variable (in this case, each of the indices).

However, non-parametric methods are recommended instead of assuming normality when analyzing time series data. The Mann–Kendall test, also known as the M–K test, is a widely used non-parametric method for identifying statistical trends, provided that the records do not exhibit persistence. This test is used to determine whether a time series exhibits a monotonic upward or downward trend. Its formula involves the sum of the signs of differences (z) for all feasible pairs, and its operational statistic *Ss* is expressed as follows (Manly, 2001):

$$Ss = \sum_{i=2}^{n}\sum_{j=1}^{i=1} sign\left(x_i - x_j\right) \tag{2}$$

Where the *sign* (z) is -1 for $z < 0$, 0 for $z = 0$, and +1 for $z > 0$. For a series consisting of random values, it is anticipated that $Ss = 0$, and its variance is determined as (Hirsch et al., 1992; Machiwal and Jha, 2012):

$$Var(Ss) = \frac{n(n-1)(2n+5)}{18} \tag{3}$$

The test statistic is:

$$Z_s = \frac{Ss + m_c}{\sqrt{Var(Ss)}} \tag{4}$$

In the last equation, $m_c = 1$ when $S_s < 0$ and $m_c = -1$ para $S_s > 0$. The series shows an increasing or decreasing trend with a significance level α if the absolute value of Z_s is greater than the critical value of the standard normal distribution. The critical value is 1.96 for α = 5%. When the data are equal or the sample is rejected, the variance must be corrected (Hirsch et al., 1992).

Conversely, Sen's slope method is a robust nonparametric technique for estimating the magnitude of a trend slope (Sen, 1968). For a given time series $X_i = x_1, x_2, \ldots, x_n$, with N pairs of data, the slope is determined as shown in Equation 5.

$$\beta_i = \frac{x_j - x_k}{j-k}, \forall k \le j \ \wedge \ i = 1, 2, \ldots \tag{5}$$

Median of N values of β_i gives the Sen's estimator of slope β.

$$\beta = \begin{cases} \frac{\beta_{N+1}}{2}, & if\ N\ isodd \\ \frac{\left(\frac{\beta_N}{2} + \frac{\beta_{N+2}}{2}\right)}{2}, & if\ N\ iseven \end{cases} \tag{6}$$

Sen's slope method was employed to evaluate the extent of change in climate change indices. This non-parametric technique utilizes a linear model to estimate the trend's slope, assuming a linear trend in the time series (Sen, 1968; Kumar et al., 2017). The Sen's slope is commonly used in the analysis of hydro-meteorological time series (Fonseca et al., 2016).

To identify significant trends in our study, we applied the Mann-Kendall (M–K) test to each time series from the climatic stations for each climate change index. Time series that did not demonstrate statistical significance were excluded from the calculations, while those that did were included.

When analyzing time series data, it is crucial to consider whether the data exhibit serial correlation. This occurs when the current value of a variable depends on its value in previous moments. The assumption of independence can be violated if there are serial correlations in time series data, which can lead to incorrect statistical results.

Therefore, for reliable and accurate results, it is essential to account for serial correlation in the analysis of time series data. The method outlined by Patakamuri et al. (2020) was utilized in this study to compute lag–1 serial correlation coefficients for evaluating the presence of serial correlation. In numerous trend studies, the time series is examined for serial correlation by calculating the lag–1 serial correlation coefficient, ρ_1. For any time series $X_i = x_1, x_2, \ldots, x_n$, the lag–1 serial correlation coefficient (ρ_1) is calculated as

$$\rho_1 = \frac{\frac{1}{n-1}\sum_{i=1}^{n-1}\left(x_i - E(x_i)\right)\cdot\left(x_{i+1} - E(x_i)\right)}{\frac{1}{n}\sum_{i=1}^{n}\left(x_i - E(x_i)\right)^2} \tag{7}$$

where $E(x_i)$ is the mean of the sample and n is the sample size

$$E(x_i) = \frac{1}{n}\sum_{i=1}^{n} x_i \quad (8)$$

The probability limits for ρ_1 on the correlogram of an independent series is given by Anderson (1941) as

$$\rho_1 = \{\frac{-1+1.645\sqrt{n-2}}{n-1}, fortheone - tailedtest\ \frac{-1\pm1.96\sqrt{n-2}}{n-1}, forthetwo - tailedtest \quad (9)$$

Significance of serial correlation was evaluated by comparing the ρ_1 value with the critical values of Student's t-distribution values.

Additional tests were conducted using Patakamuri tests, if the time series showed evidence of serial correlation. However, if the time series did not exhibit serial correlation, it was retained as a statistically significant time series. As a result, the final trends were calculated using this time series. The M–K trend test alone is inadequate when dealing with time series data exhibiting serial correlation.

This study used a method that does not have a universal approach to determine the presence of serial correlation in time series data. Patakamuri et al. (2020) described five statistical tests that supported the method used: the first is the pre-whitened M–K test (Von Storch & Navarra, 1995); the trendless pre-whitened M–K test (Yue et al., 2002); the bias correction applied to pre-whitening (Hamed, 2009); the variance correction approach proposed by Hamed & Rao (1998); and the variance correction approach proposed by Yue & Wang (2004). The time series was considered significant, if at least three of these tests produced statistically significant results with at least 95% confidence. However, if fewer than three tests were significant, the time series was considered non-significant and excluded from further calculations.

The Patakamuri tests mentioned above are described as follows:

- Pre-whitened M–K test

For a given time series $X_i = x_1, x_2, \ldots, x_n$, with lag–1 serial correlation coefficient ρ_1 as mentioned in Equation (5), pre-whitened series X_t' is given by von Storch (1995) as

$$X_t' = X_t - \rho_1 X_{t-1} \quad (10)$$

- Trend-free pre-whitened M–K test

In the trend-free pre-whitening (Yue et al., 2002) of a given time $X_t = x_1, x_2, \ldots, x_n$, the first step involves calculating the Sen's slope using Equations (5) and (6). The monotonic trend β is then removed from X_i to create a trend-free series y_t

$$y_t = x_t - \beta t \quad (11)$$

where x_t is the series value at time t, y_t is the detrended series, and β is the trend slope.

In the next step, the lag–1 serial correlation coefficient ρ_1 of the detrended series y_t is calculated as described in Equation (7). If ρ_1 is not significant, trend detection is conducted on the detrended series. If there is significant serial correlation at lag–1, the de-trended series is pre-whitened, and the residual series is computed as follows

$$y_t' = y_t - \rho_1 y_{t-1} \quad (12)$$

In the final stage, the monotonic trend component is added back to residual series y_t' to generate the trend-free pre-whitening series X_t

$$X_t = y_t' + \beta t \quad (13)$$

- Bias correction applied to pre-whitening

A time series $X_t = x_1, x_2, \ldots, x_n$, which is presumed to follow a first-order serial correlation process with an included linear trend, can be represented as follows:

$$X_t = \rho X_{t-1} + \alpha + \beta t + \varepsilon_t \quad (14)$$

where X_t and X_{t-1} are observations at times t and t - 1, respectively; ρ is the serial correlation coefficient; α is constant intercept term; β is trend slope with respect to time; and ε_t is an uncorrelated noise term. The estimated values of ρ, α and β are given by

$$[\rho\ \alpha\ \beta]^T = (Z^T Z)^{-1} Z^T y \quad (15)$$

where Z is the matrix of size n - 1 · 3 whose second column contains (n - 1) values equal to 1, and the third column contains the numbers 2 to n and y is a vector of size (n - 1) · 1 containing the observations x_2 to x_n. The bias-corrected serial correlation coefficient ρ [45,86] is calculated using the formula mentioned in Equation (16). This value is used in bias-corrected pre-whitening and trend detection studies.

$$\rho = \frac{(n\rho' + 2)}{n-4} \quad (16)$$

- Variance correction approaches

In a time series $X_t = x_1, x_2, \ldots, x_n$, with n observations, the effective information is contained in n observations, where n is always less than the original sample size n. Positive or negative serial correlation causes the variance of the M–K test statistic S to increase or decrease, respectively. To mitigate this effect, the modified variance $V(S)$ is calculated by

$$V(S) = V(S) \times CF \quad (17)$$

Correction factors (CF) proposed by Hamed and Rao (1998) and Yue and Wand (2004) termed as CF_1 and CF_2, respectively are

$$CF_1 = 1 + \frac{2}{n(n-1)(n-2)}\sum_{k=1}^{n-1}(n-k)(n-k-1)(n-k-2)r_k^R \quad (18)$$

$$CF_2 = 1 + 2\sum_{k=1}^{n-1}\left(1 - \frac{k}{n}\right)r_k \quad (19)$$

where r_k and r_k^R are the lag –k serial correlation coefficients of data and ranks of data respectively and n is the total length of the series. In the case of CF_1 only significant correlation coefficients are used. For calculating CF_2, lag - 1 serial correlation coefficient is used. The M–K trend test is calculated by using corrected variance $v(s)$.

4. Results and discussion

26 indices were obtained from those listed in Table 1, to which a linear adjustment was applied to obtain the trend, following equation (1). It is noted that the data represents time series in an annual window. Figures 2 and 3 correspond to the evolution of the dtr, gddgrow10, tmm, tn10, and tn90p indices, respectively, over the period 1940-2022. The remaining plots can be found in Annex B.

Statistical tests were applied to determine the significance of the trends and obtain the significant trend based on them using the Sen's slope (see the methodology section). Figure 4 shows the indices that exhibited a significant trend.

This study demonstrated the adjustment of significant trends that passed statistical tests for temperature-related climate indices. Out of these, two exhibited a negative trend (tn10p and tx10p). These indices indicate minimum and maximum temperatures below the 10th percentile, suggesting a decrease in cold temperature days. Specifically, tn10p refers to cold nights in comparison to the reference period, while tx10p relates to cold days in the region where the daily maximum temperature falls below the annual or monthly threshold relative to the baseline period.

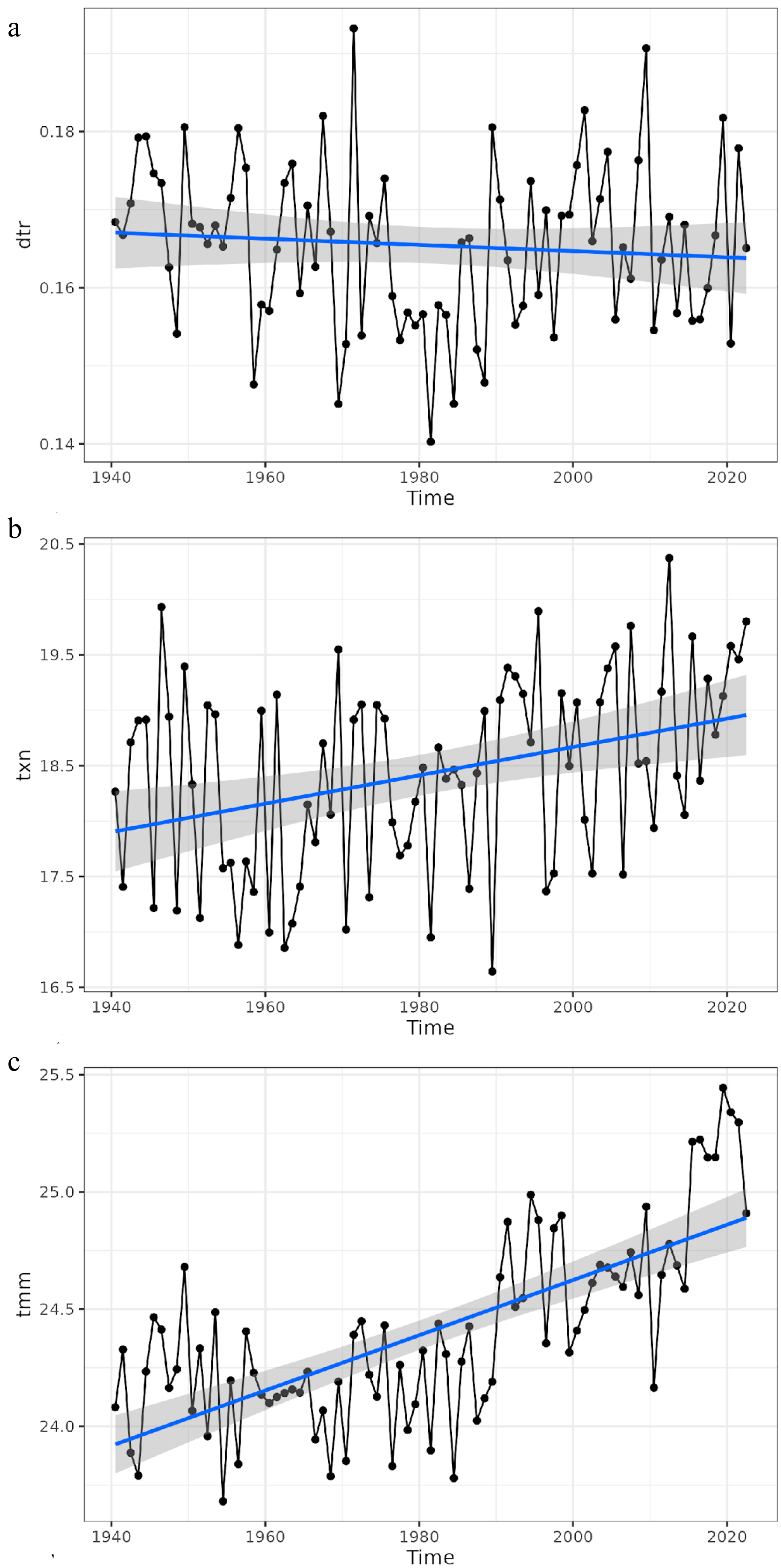

Figure 2. Annual time series of the climate change indices in black. In blue is the linear fit (see table 2). The gray area is the associated standard error. a) dtr (°C), b) txn (°C), c) tmm (°C).

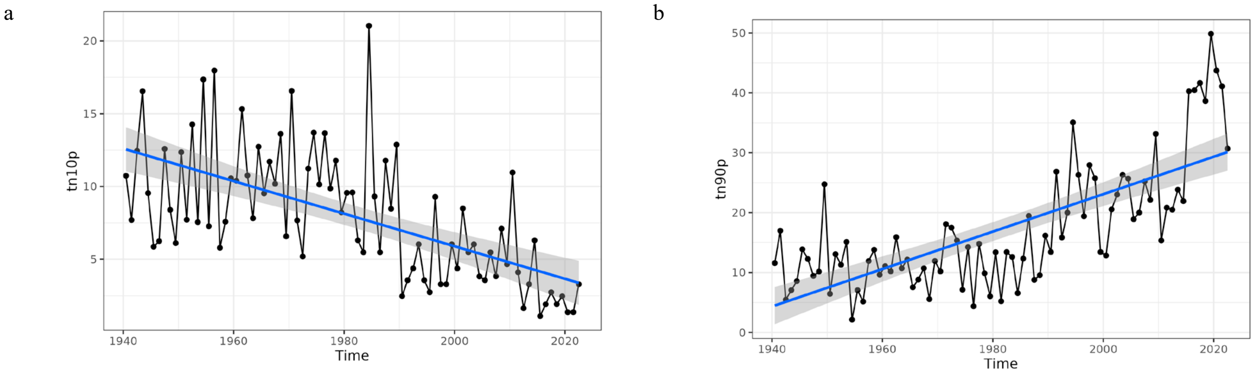

Figure 3. The same as in Figure 2 but for the a) tn10p (%) and b) tn90p (%) climate change indices.

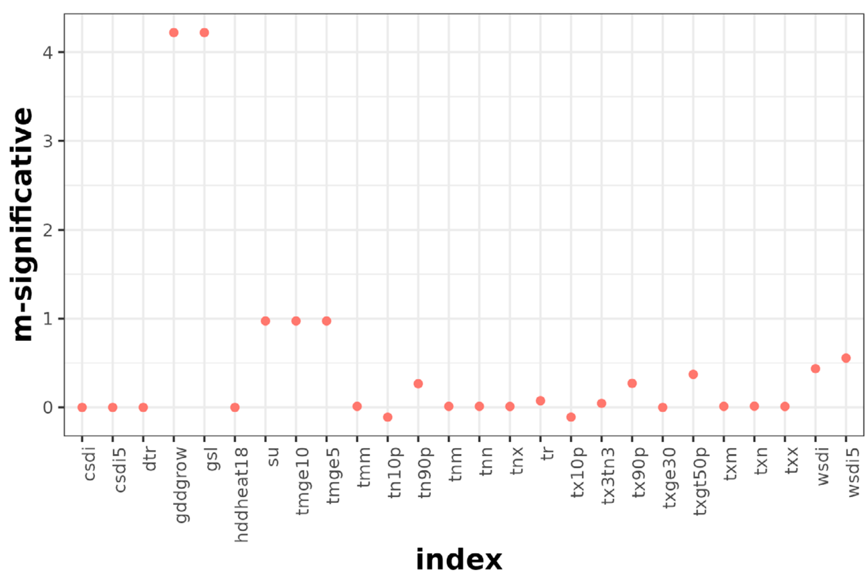

Figure 4. Indices with significant trends (see Table 2).

Table 2. List of significant trends (significant M) after applying statistical tests and Sen's slope. Y (linear fit) and its R^2. Additionally, the extrapolated value of 2023 (*Note: this value is taken from the linear fit, however the M is significant to determine it as null)

Climate change Index	M significative	Y (linear fit)	R^2	2023 extrapolated value
csdi5	0 (days/yr)	$y = 4.82 - 2.09 * 10^{-4}\,x$	0.12	4.40 days *
csdi	0 (days/yr)	$y = 2{,}85 - 1.28 * 10^{-4}\,x$	0.07	2.60 days *
dtr	0 (°C/yr)	$y = 0.166 - 1.08 * 10^{-7}\,x$	<0.01	0.166 °C*
gddgrow	4.22 (°C days/yr)	$y = 5.21 * 10^{+3} + 1.18 * 10^{-2}\,x$	0.50	545 (°C days)
gsl	4.22 (days/yr)	$y = 365 - 1.21 * 10^{-6}\,x$	<0.01	365 (days)
hddheat18	0 (°C days/yr)	$y = 482 - 2.11 * 10^{-5}\,x$	0.05	482 (°C days)*
su	0.97 (days/yr)	$y = 146 + 2.66 * 10^{-3}\,x$	0.55	151 (days)
tmge10	0.97 (days/yr)	$y = 365 - 1.21 * 10^{-6}\,x$	<0.01	365 (days)
tmge5	0.97 (days/yr)	$y = 365 - 1.21 * 10^{-6}\,x$	<0.01	365 (days)
tmm	0.01 (°C/yr)	$y = 24.3 + 3.22 * 10^{-5}\,x$	<0.5	24.36 (°C)
tn10p	-0.11 (%/yr)	$y = 9.25 - 3.06 * 10^{-4}\,x$	<0.38	9.63 (%)
tn90p	0.27 (%/yr)	$y = 13.7 + 8.56 * 10^{-4}\,x$	0.53	15.43 (%)
tnm	0.01 (°C/yr)	$y = 24.2 + 3.23 * 10^{-5}\,x$	0.50	24.26 (°C)
tnn	0.01(°C/yr)	$y = 18.1 + 3.19 * 10^{-5}\,x$	0.10	18.16 (°C)
tnx	0.01(°C/yr)	$y = 28.7 + 3.02 * 10^{-5}\,x$	0.19	28.76 (°C)
tr	0.07 (days/yr)	$y = 354 + 1.86 * 10^{-4}\,x$	0.07	354 (days)

(*Continued*)

Climate change Index	M significative	Y (linear fit)	R^2	2023 extrapolated value
tx10p	-0.11 (%/yr)	$y = 9.22 - 3.01 * 10^{-4} x$	0.38	8.61 (%)
tx3tn3	0.05 (events/yr)	$y = 1.16 + 1.85 * 10^{-4} x$	0.42	1.53 (%)
tx90p	0.27 (%/yr)	$y = 13.7 + 8.51 * 10^{-4} x$	0.53	15.42 (%)
txb3tnb3	NA	$y = 0.517 - 1.71 * 10^{-5} x$	0.05	0.482
txge30	0 (days/yr)	$y = 6.86*10^{-2} + 9.48 * 10^{-6} x$	0.02	686 (days)*
txgt50p	0.37 (%/yr)	$y = 54.4 + 1.00 * 10^{-3} x$	0.49	56.4 (%)
txm	0.01(°C/yr)	$y = 24.4 + 3.22 * 10^{-5} x$	0.50	24.5 (°C)
txn	0.01(°C/yr)	$y = 18.3 + 3.5 * 10{-}5\ x$	0.12	18.4 (°C)
wsdi5	0.56 (days/yr)	$y = 13.4 + 2.16 * 10^{-3} x$	0.47	17 (days)
wsdi	0.44(days/yr)	$y = 10 + 1.83 * 10^{-3} x$	0.44	13 (days)

On the other hand, the gddgrow and gsl indices show positive trends with values exceeding 4 (days/year). Gddgrow is an index indicating the accumulation of heat for plant growth, while gsl denotes the annual duration of warm days. This implies that, in both cases, warm days have been increasing rapidly.

A trend of 1 (days/year) is observed for the su, tmge10, and tmge5 indices. The first corresponds to summer days, and the other two relate to average temperatures above 10 and 5 °C, respectively. These indices show an increase in recent years. Additionally, there is a slightly lower, but positive trend of less than 0.5 (units/year) for the tn90p (%), tx90p (%), tr (days), txgt50p (%), and wsdi (days) indices, indicating an increase in maximum temperatures, tropical nights, and maximum temperature.

While the rest of the indices showed a trend with the linear adjustment, when statistical tests were applied, their trends are reported in Table 2. We can see that the indices tmm, tnm, tnn, tnx, txn, txm, and txx exhibit a trend of 0.01°C/yr. These results are in agreement with previous studies in the region (Cavazos et al., 2020; Andrade-Velázquez et al., 2021). On the other hand, there were 5 indices (csdi, csdi5, dtr, hddheat18, txge30p) with a trend of zero, meaning they do not show an increasing or decreasing pattern. Additionally, there was only one climate change index in which its trend was not statistically significant, and that is the case of txb3tnb3.

However, the indices that showed a significant trend indicate the detection of local warming and, therefore, climate change (IPCC, 2012). Zarazúa-Villaseñor et al., (2014) calculated climate change indices for various coastal areas south of the Gulf of Mexico in the period 1961-2007. They reported an increase in hot days and warm nights in Paraíso. Therefore, we suggest that the climate change indices presented in this study can be used as standard markers for detecting climate change in the study area. It is worth noting that these indices are used in the Energy, Agriculture, Food Security, Coastal, Health, and Environmental sectors (CLIMPACT, 2023). Globally, several studies have applied climate change indices to monitor changes in climate extremes. They have also been used in regional analyses (Montero-Martínez et al., 2022).

This study determines climate change indices for the coastal area of Paraíso, Tabasco municipality, where the LANRESC Coastal Resilience Observatory is located. These indices indicate a continuous increase in temperatures in recent years. The resulting impacts primarily affect the comfort of the population and will have a more significant impact on vulnerable sectors, such as the elderly and children, who make up 27% of the population in the area, according to INEGI (2021). The federal government (COFEPRIS, 2023) has reported health effects due to the presence of heatwaves. Another effect of rising temperatures is the growing demand for water for consumption and productive activities (INEGI, 2017). Escudero & Mendoza (2021) report that Tabasco is among the states affected by climate change in terms of livelihoods, health, and local subsistence. Jiménez-Hernández et al. (2021) state that populations in the Gulf of Mexico coasts are migrating due to climate change events, and the communities' infrastructure is vulnerable to these events. However, it is important to note that human settlements along the Paraíso coast have recently increased due to oil-related activities, which exposes a larger population to climate change.

On the other hand, the stress experienced by ecosystems due to warming in the study area endangers wildlife species (Yáñez-Arancibia & Day, 2010). Sauz-Sánchez et al. (2021) report that increasing temperatures may lead to the displacement of fish to other regions in land. Andrade-Velázquez & Montero-Martínez (2023) demonstrate that temperatures have been rising at a rate of 0.025°C per year in southeastern Mexico, and this trend may continue through the year 2021-2040 under the SSP4-6.0 scenario. Additionally, Andrade-Velázquez et al. (2021) report that the southeastern region of Mexico, Central America, and the Caribbean are experiencing a similar continental warming trend (0.10-0.2°C per year). NCEI (2023) reports an increase in the temperature of the Gulf of Mexico. Sanchez-García et al. (2017) suggest that this could alter currents in the southern Gulf of Mexico, affecting species and serving as an indicator of warming. On the other hand, the rising temperature in the marine influence zone will create favorable conditions for the formation of more tropical cyclones. While their trajectories cannot be predicted with certainty, it is likely that there will be greater impacts in the area (Dominguez et al., 2021; Appendini & Ruiz-Salcines, 2022).

It is important to highlight that the OCR-Tabasco is a socioecosystem, composed of multiple subsystems with different variables that interact with each other, making it a complex system, in accordance with the ecosystem definition by Ostrom (2009), Liu et al. (2007), and Vidal-Hernández et al. (2020). According to Rodríguez-Fuentes et al. (2020), there are two types of stressors that can impact socioecosystems, exogenous ones (which generate changes) and endogenous ones (inherent). Climate-related changes fall under the exogenous category. Thus, climate change indices are measures of these stressors affecting the OCR and its historical trajectory to determine its resilience (Ávila-Foucat et al., 2020). Furthermore, these indices allow us to provide quantifiable information about the climate to address climate change and its effects, aligning with Goal 13, "Climate Action," of the 17 Sustainable Development Goals (ONU, 2023).

In the mind map, the climate change indices trends for the OCR-Tabasco are represented from the significant M. In this graph, the (percentiles) climate change indices show trends, while the other indices remain close to zero. The local area is warming, as reported by Aguilar et al. (2005) for southern Mexico, and by Andrade-Velázquez et al. (2021) and Andrade-Velázquez and Montero-Martínez (2023).

These results help determine the climate change impacts that are occurring and could occur in the study area. The socio-ecosystem is facing increasing warming; if this warming is not addressed with mitigation actions, the population will suffer more health impacts. In addition, adaptation actions in the socio-ecosystem must be applied now to conserve various communities and strengthen socio-ecosystem resilience. The vulnerability of coastal areas is also evident due to warming, not only because of coastal erosion but also the rising sea levels.

Conclusions

This study reports, for the first time, an analysis of 26 climate change indices for the municipality of Paraíso, Tabasco, which includes the Dos Bocas Port in Tabasco and the Coastal Resilience Observatory of LANRESC. The information presented reveals increasing trends in the indices of gddgrowq, gsl, su, tmge10, tmge5, tn90p, tr, tx90p, txgt50p, wsdi, and swdi5. The indices that show decreases are tn10p and tx10p, which correspond to cold temperatures in the study area. All these indices reflect local warming and the detection of Climate Change, in accordance with the World Meteorological Organization and the IPCC (IPCC, 2012).

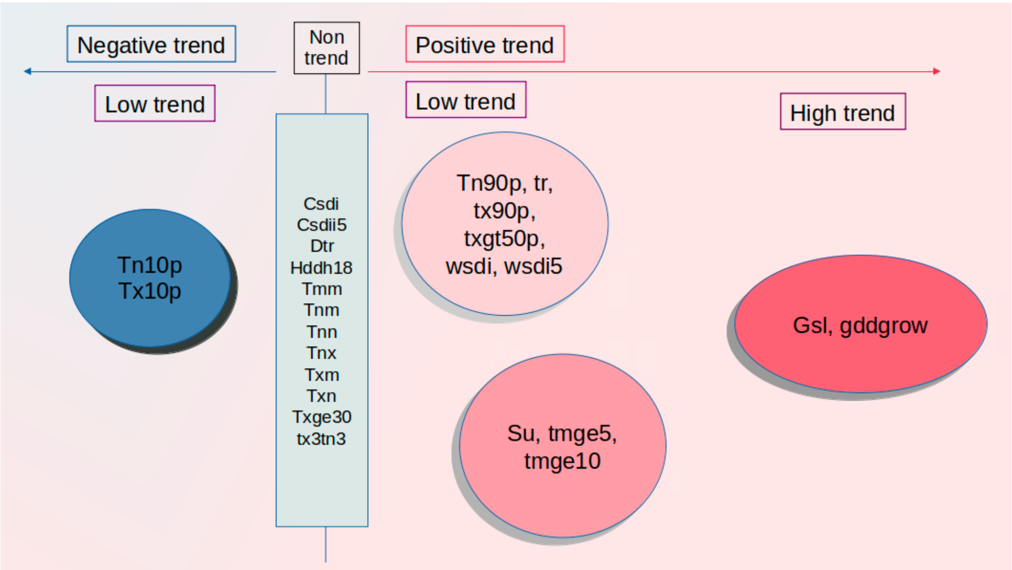

Figure 5. Mind Map on the trends of climate indices. Red indicates indices with a positive trend, blue indicates a negative trend, and green indicates a trend close to zero. See table 1 for the climate change indices names.

This study is the first to apply the methodology of climate change indices with statistical significance tests, following Montero-Martínez & Andrade-Velázquez (2022). The intention is to replicate this approach in the other 6 OCRs of LANRESC. It is worth noting that there is not much literature on this topic for coastal areas in Mexico, especially in the study area. The significance of this site is regional, given its volume of cargo and vessels, as it is a port. Additionally, it is home to the refinery owned by Petróleos Mexicanos (PEMEX). Therefore, this study serves as a reference for future environmental and social research seeking information on climate change events in the study area.

Acknowledgments

To the *Investigadores por México* program, formerly *Cátedras-CONAHCYT*, particularly to project 945. To Dr. Paullo Salles and Dr. Gema Hidalgo of the *Laboratorio Nacional de Resiliencia Costera* (LANRESC). To the networks in Mexico: REDESClim, UGM and LANCAC.

References

Adams, S. R. (1999). *Recuperación con mangle blanco (Laguncularia racemosa) de áreas impactadas por hidrocarburos y su manejo como agrosilvo-ecosistema en la zona costera de Huimanguillo y Cárdenas, Tabasco.* México. Universidad Juárez Autónoma de Tabasco. Available online: http://www.conabio.gob.mx/institucion/proyectos/resultados/InfM076.pdf (last accessed August 2024)

Aguilar, E., Peterson, T. C., Obando, P. R., Frutos, R., Retana, J. A., Solera, M., Soley, J., García, I. G., Araujo, R. M., Santos, A. R., Valle, V. E., Brunet, M., Aguilar, L., Álvarez, L., Bautista, M., Castañón, C., Herrera, L., Ruano, E., Sinay, J. J., . . . Mayorga, R. (2005). Changes in precipitation and temperature extremes in Central America and northern South America, 1961-2003. *Journal of Geophysical Research: Atmospheres*, 110(D23). https://doi.org/10.1029/2005JD006119

Alizad, K., Hagen, S. C., Medeiros, S. C., Bilskie, M. V., Morris, J. T., Balthis, L., & Buckel, C. A. (2018). Dynamic responses and implications to coastal wetlands and the surrounding regions under sea level rise. *PloS one*, 13(10), e0205176. https://doi.org/10.1371/journal.pone.0205176

Anderson, R. L. (1942). Distribution of the Serial Correlation Coefficient. *The Annals of Mathematical Statistics*, 13, 1–13.

Andrade-Velázquez, M. (2017). Visión climática de la precipitación en la cuenca del Río Usumacinta. In: Soares, D., & García, G. A. (Eds.). *La Cuenca del Río Usumacinta desde la Perspectiva del Cambio Climático.* Instituto Mexicano de Tecnología del Agua: Jiutepec, México, 1-417.

Andrade-Velázquez, M., Medrano-Pérez, O. R., Montero-Martínez, M. J., & Alcudia-Aguilar, A. (2021). Regional Climate Change in Southeast Mexico-Yucatan Peninsula, Central America and the Caribbean. *Applied Sciences,* 11(18), 8284. https://doi.org/10.3390/app11188284

Andrade-Velázquez, M., & Montero-Martínez, M. J. (2023). Historical and Projected Trends of the Mean Surface Temperature in South-Southeast Mexico Using ERA5 and CMIP6. *Climate*, 11, 111. https://doi.org/10.3390/cli11050111

Aparicio, J., Martínez-Austria, P. F., Güitrón, A., & Ramírez, A. I. (2009). Floods in Tabasco, Mexico: a diagnosis and proposal for courses of action. *Journal of Flood Risk Management*, 2(2), 132-138. https://doi.org/10.1111/j.1753-318X.2009.01026.x

Appendini, C. M., & Ruiz-Salcines, P. (2022). Oleaje y diseño de estructuras marítimas en zonas tropicales bajo el contexto del cambio climático. *Gaceta Instituto de Ingeniería, UNAM,* 1(152), 16-19. Available online: https://www.iingen.unam.mx/es-mx/AlmacenDigital/Gaceta/Gaceta-enero-febrero-2022/Paginas/oleaje-diseno-estructuras-maritimas.aspx (last accessed: August 2024).

Ávila-Foucat, S., Torres-Freyermuth, A., Esqueda-Lara, K., Medellín-Mayoral, G., Salgado-Nieto, U., González-Quintero, C., Ramírez-León A., Reyna-Fabián, M. (2020). Trayectoria de los socioecosistemas costeros. In: Ávila-Foucat, S., & Espejel, I.(Eds.). *Resiliencia de Socioecosistemas Costeros.* Primera Edición. UNAM. ISBN: 978-607-30-3164-6, 190 pp.

Arreguín-Cortés, F. I., Rubio-Gutiérrez, H., Domínguez-Mora, R., & Luna-Cruz, F. D. (2014). Análisis de las inundaciones en la planicie tabasqueña en el periodo 1995-2010. *Tecnología y Ciencias del Agua*, 5(3), 5-32. https://revistatyca.org.mx/index.php/tyca/article/view/424

Cavazos, T., Luna-Niño, R., Cerezo-Mota, R., Fuentes-Franco, R., Méndez, M., Pineda Martínez, L. F., & Valenzuela, E. (2020). Climatic trends and regional climate models intercomparison over the CORDEX-CAM (Central America, Caribbean, and Mexico) domain. *International Journal of Climatology*, 40(3), 1396-1420. https://doi.org/10.1002/joc.6276

CENAPRED. (2021). *Impacto socioeconómico de los principales desastres ocurridos en México. Resumen ejecutivo 2020*. Secretaría de Seguridad y Protección Ciudadana. Centro Nacional de Prevención de Desastres. https://www.cenapred.unam.mx/es/Publicaciones/archivos/455-RESUMENEJECUTIVOIMPACTO2020.PDF (last accessed: August 2024).

CLIMPACT. (2023). https://climpact-sci.org/ (last accessed: August 2024).

COFEPRIS. (2023). Comisión Federal para la Protección de Riesgos Sanitarios. https://www.gob.mx/cofepris/acciones-y-programas/efectos-del-cambio-climatico-y-los-riesgos-derivados-para-la-salud (last accessed: August 2024).

Colorado-Ruiz, G., & Cavazos, T. (2021). Trends of daily extreme and non-extreme rainfall indices and intercomparison with different gridded data sets over Mexico and the southern United States. *International Journal of Climatology,* 41(11), 5406–5430. https://doi.org/10.1002/joc.7225

CONABIO. (2023). Comisión Nacional de la Biodiversidad. https://www.gob.mx/conabio (last accessed: August 2024).

Dominguez, C., Jaramillo, A., & Cuéllar, P. (2021). Are the socioeconomic impacts associated with tropical cyclones in Mexico exacerbated by local vulnerability and ENSO conditions? *International Journal of Climatology*, 41, E3307-E3324. https://doi.org/10.1002/joc.6927

Escudero, M., & Mendoza, E. (2021). Community Perception and Adaptation to Climate Change in Coastal Areas of Mexico. *Water*, 13(18), 2483. https://doi.org/10.3390/w13182483

Fonseca, D., Carvalho, M. J., Marta-Almeida, M., Melo-Gonçalves, P., & Rocha, A. (2016). Recent trends of extreme temperature indices for the Iberian Peninsula. *Physics and Chemistry of the Earth, Parts A/B/C*, 94, 66-76. https://doi.org/10.1016/j.pce.2015.12.005

Gama, L., Ordoñez, E. M., Villanueva-García, C., Ortiz-Pérez, M. A., López, H. D., Torres, R. C., & Valadez, M. E. M. (2010). Floods in Tabasco Mexico: history and perspectives. In: Wrachien, D. & Proverbs, D. (Eds). *Flood Recovery, Innovation and Response II*. WIT Transactions on Ecology and the Environment https://doi.org/10.2495/FRIAR100031

García-López, E., Zavala-Cruz, J., & Palma-López, D. J. (2006). Caracterización de las comunidades vegetales en un área afectada por derrames de hidrocarburos. *Terra Latinoamericana*, 24(1), 17-26. https://www.redalyc.org/articulo.oa?id=57311494003

Hamed, K. H., & Rao, A. R. (1998). A modified Mann-Kendall trend test for autocorrelated data. *Journal of Hydrology*, 204(1-4), 182-196. https://doi.org/10.1016/S0022-1694(97)00125-X

Hamed, K. H. (2009). Enhancing the effectiveness of prewhitening in trend analysis of hydrologic data. *Journal of Hydrology*, 368(1-4), 143-155. https://doi.org/10.1016/j.jhydrol.2009.01.040

Hernández Melchor, G. I., Ruíz Rosado, O., Sol Sánchez, Á., & Valdez Hernández, J. I. (2017). Cambios De Uso Del Suelo En Manglares De La Costa De Tabasco. *Revista Mexicana De Ciencias Agrícolas*, 7(SPE14), 2757-2767. https://doi.org/10.29312/remexca.v0i14.444

Hernández Santana, J. R., Ortiz Pérez, M. A., Méndez Linares, A. P., & Gama Campillo, L. (2008). Morfodinámica de la línea de costa del estado de Tabasco, México: tendencias desde la segunda mitad del siglo XX hasta el presente. *Investigaciones Geográficas*, 65, 7-21.

Hersbach, H., Bell, B., Berrisford, P., Biavati, G., Horányi, A., Muñoz Sabater, J., ... & Rozum, I. (2018). ERA5 hourly data on pressure levels from 1940 to present. *Copernicus Climate Change Service (C3S) Climate Data Store (CDS)*. https://doi.org/10.24381/cds.bd0915c6

Hirsch, R. M., Helsel, D. R., Cohn, T. A., & Gilroy, E. J. (1992). *Statistical analysis of hydrologic data*. Handbook of Hydrology, 17-55.

INEGI. (2017). *Anuario estadístico y geográfico de Tabasco 2017*. Instituto Nacional de Estadística y Geografía.-- México : INEGI, c2017. 440 p.

INEGI. (2021).. *Censo de Población y Vivienda (2020). Panorama sociodemográfico de Tabasco: Censo de Población y Vivienda 2020*. CPV /Instituto Nacional de Estadística y Geografía.--México : INEGI, c2021.

INEGI. (2023). Instituto Nacional de Estadística y Geografía. Información por entidad. Tabasco, México. https://cuentame.inegi.org.mx/monografias/informacion/tab/territorio/clima.aspx?tema=me&e=27 (last accessed: August 2024).

IPCC. (2012). *Managing the Risks of Extreme Events and Disasters to Advance Climate Change Adaptation. A Special Report of Working Groups I and II of the Intergovernmental Panel on Climate Change*. Cambridge University Press, The Edinburgh Building, Shaftesbury Road, Cambridge CB2 8RU ENGLAND, 582 pp.

IPCC, (2022). *Climate Change 2022: Impacts, Adaptation, and Vulnerability. Contribution of Working Group II to the Sixth Assessment Report of the Intergovernmental Panel on Climate Change*. Cambridge University Press, Cambridge, UK and New York, NY, USA, 3056 pp., https://doi.org/10.1017/9781009325844

Jiménez-Hernández, S. B., Pérez Montero, O., Meza, E., Velázquez, Y. R., Castellanos, J. R., Martínez-Cano, E., ... & Milanes, C. B. (2021). Coastal Migration Index for Coastal Flooding Events Increased by Sea Level Rise due to Climate Change: Mexico and Cuba Case Studies. *Water*, 13(21), 3090. https://doi.org/10.3390/w13213090

Kumar, N., Panchal, C. C., Chandrawanshi, S. K., & Thanki, J. D. (2017). Analysis of rainfall by using Mann-Kendall trend, Sen's slope and variability at five districts of south Gujarat, India. *Mausam*, 68, 205–222. https://doi.org/10.54302/mausam.v68i2.604

LANRESC. (2023). Laboratorio Nacional de Resiliencia Costera. https://www.lanresc.mx/ (last accessed: August 2024).

Liu, J., Dietz, T., Carpenter, S. R., Alberti, M., Folke, C., Moran, E., ... & Taylor, W. W. (2007). Complexity of coupled human and natural systems. *Science*, 317(5844), 1513-1516. https://doi.org/10.1126/science.1144004

Machiwal, D., & Jha, M. K. (2012). *Hydrologic Time Series Analysis: Theory and Practice*. Springer Science & Business Media.

Manly, B. F. J. (2001). *Statistics for Environmental Science and Management.* Chapman & Hall/CRC Press.

Mata-Zayas, E. E., Gama, L., Vazquez-Navarrete, C., Diaz-Lopez, H., Figueroa-Maheng, J. M., & Rincón-Ramírez, J. (2017). Vulnerabilidad de los servicios ecosistémicos en la zona de influencia costera de la Reserva de la Biosfera Pantanos de Centla, ante la elevación de nivel medio del mar asosciada al cambio climático. *Vulnerabilidad de las zonas costeras de Latinoamérica al cambio climático*, 193-230.

Montero-Martínez, M. J., Santana-Sepúlveda, J. S., Pérez-Ortiz, N. I., Pita-Díaz, Ó., Castillo-Liñan, S. (2018). Comparing climate change indices between a northern (arid) and a southern (humid) basin in Mexico during the last decades. *Advances in Science and Research,* 15, 231–237. https://doi.org/10.5194/asr-15-231-2018

Montero-Martínez, M. J., Pita-Díaz, O., & Andrade-Velázquez, M. (2022). Potential Influence of the Atlantic Multidecadal Oscillation in the Recent Climate of a Small Basin in Central Mexico. *Atmosphere*, 13, 339. https://doi.org/10.3390/atmos13020339

Montero-Martínez, M. J., & Andrade-Velázquez, M. (2022). Effects of Urbanization on Extreme Climate Indices in the Valley of Mexico Basin. *Atmosphere*, 13(5), 785. https://doi.org/10.3390/atmos13050785

NCEI (2023). *The Gulf of Mexico Is Getting Warmer.* National Centers for Environmental Information. National Oceanic and Atmospheric Administration. https://www.ncei.noaa.gov/news/gulf-mexico-getting-warmer (last accessed: August 2024).

ONU. (2023). *Objetivos de Desarrollo Sostenible*. Organización de las Naciones Unidas. https://www.un.org/sustainabledevelopment/es/objetivos-de-desarrollo-sostenible/ (last accessed: August 2024).

Ostrom, E. (2009). A general framework for analyzing sustainability of social-ecological systems. *Science*, 325(5939), 419-422.

Patakamuri, S. K., Muthiah, K., & Sridhar, V. (2020). Long-term homogeneity, trend, and change-point analysis of rainfall in the arid district of Ananthapuramu, Andhra Pradesh State, India. *Water*, 12(1), 211. https://doi.org/10.3390/w12010211

Peterson, T. C., Zhang, X., Brunet-India, M., & Vázquez-Aguirre, J. L. (2008). Changes in North American extremes derived from daily weather data. *Journal of Geophysical Research: Atmospheres,* 113(D7). https://doi.org/10.1029/2007JD009453

Perevochtchikova, M., & Lezama de la Torre, J. L. (2010). Causas de un desastre: inundaciones del 2007 en Tabasco, México. *Journal of Latin American Geography,* 9(2), 73-98.

Pita-Díaz, O., & Ortega-Gaucin, D. (2020). Analysis of Anomalies and Trends of Climate Change Indices in Zacatecas, Mexico. *Climate,* 8(4), 55. https://doi.org/10.3390/cli8040055

Rastogi, R. P., Phulwaria, M., & Gupta, D. K. (2021). *Mangroves: Ecology, biodiversity and management.* Springer Singapore. https://doi.org/10.1007/978-981-16-2494-0

Rodríguez-Fuentes, G., Reyna-Fabián, M., Pérez-Espejo, R., Jiménez-Orocio, O. A., Ávila-Foucat, S., & Espejel, I. (2020). Estresores de los socioecosistemas costeros y variables para su medición en Resiliencia de Socioecosistemas Costeros, coordinadoras Ávila-Foucat, S. & Espejel, I. (Eds). *Resiliencia de socioecosistemas costeros.* Primera Edición. UNAM. ISBN: 978-607-30-3164-6, 190 pp.

Sanchez-García, A., Rodríguez-Fuentes, G., Díaz, F., Galindo-Sánchez, C. E., Ortega, K., Mascaró, M., ... & Rosas, C. (2017). Thermal sensitivity of O. maya embryos as a tool for monitoring the effects of environmental warming in the Southern of Gulf of Mexico. *Ecological Indicators*, 72, 574-585. https://doi.org/10.1016/j.ecolind.2016.08.043

Sandilyan, S., & Kathiresan, K. (2014). Decline of mangroves–a threat of heavy metal poisoning in Asia. *Ocean & Coastal Management*, 102, 161-168. https://doi.org/10.1016/j.ocecoaman.2014.09.025

Sauz-Sánchez, J. D. J., Rodiles-Hernández, R., Andrade-Velázquez, M., Mendoza-Carranza, M. (2021). Modelling the potential distribution of two tropical freshwater fish species under climate change scenarios. *Aquatic Conservation: Marine and Freshwater Ecosystems*, 31(10), 2737-2751. https://doi.org/10.1002/aqc.3663

SEDEC. (2023). *Perfil del Estado de Tabasco.* Subsecretaría de Promoción y Atracción de Inversiones. Dirección de Inversión y Fomento Industrial. Secretaría de Desarrollo Económico y la Competitividad.

SEMAR. (2023). *Dos Bocas, Tabasco.* Secretaría de Marina. Available online: https://digaohm.semar.gob.mx/derrotero/cuestionarios/cnarioDosbocas.pdf (last accessed: August 2024).

SEMARNAP. (1997). *Primera Comunicación Nacional ante la Convención Marco de las Naciones Unidas sobre el Cambio Climático*. Secretaría de Medio Ambiente, Recursos Naturales y Pesca. https://www.gob.mx/cms/uploads/attachment/file/666956/Primera_Comunicaci_n_Nacional.pdf (last accessed: August 2024).

Sen, P. K. (1968). Estimates of the regression coefficient based on Kendall's Tau. *Journal of the American Statistical Association,* 63, 1379–1389. https://doi.org/10.1080/01621459.1968.10480934

SMN. (2023). *Normales Climatológicas.* Servicio Meteorológico Nacional. https://smn.conagua.gob.mx/es/climatologia/informacion-climatologica/mapas-de-climatologia-1981-2010 (last accessed: August 2024).

Vidal-Hernández, L. E., Ávila-Foucat, S., Arce-Ibarra, M., Tovilla-Hernández, C., & Carmona-Escalante, A. (2020). Construcción de socioecosistemas costeros para medir su resiliencia. In: Ávila-Foucat, S., & Espejel, I. (Eds.) *Resiliencia de Socioecosistemas Costeros*. Primera Edición. UNAM. ISBN: 978-607-30-3164-6, 190 pp.

Von Storch, H., & Navarra, A. (1995). Misuses of Statistical Analysis in Climate Research. In: Storch, H., & Navarra, A. (Eds). *Analysis of Climate Variability-Applications of Statistical Techniques*. Springer: Berlin/Heidelberg, Germany; pp. 11–26.

WMO. (2018). *Commission for Climatology.* Organización Meteorológica Mundial. https://library.wmo.int/viewer/56004?medianame=1216_en_#page=1&viewer=picture&o=download&n=0&q= (last accessed: August 2024).

Yáñez-Arancibia, A., & Day, J. W. (2010). La zona costera frente al cambio climático: vulnerabilidad de un sistema biocomplejo e implicaciones en el manejo costero. In: Rivera-Arriaga, E., Azuz-Adeath, I., Alpuche Gual, L., & Villalobo-Zapata, G. J. (Eds). *Cambio Climático en México un Enfoque Costero-Marino*. Universidad Autónoma de Campeche Cetys-Universidad, Gobierno del Estado de Campeche. 944 p.

Yue, S., Pilon, P., Phinney, B., & Cavadias, G. (2002). The influence of autocorrelation on the ability to detect trend in hydrological series. *Hydrological Processes*, 16(9), 1807-1829. https://doi.org/10.1002/hyp.1095

Yue, S., & Wang, C. (2004). The Mann–Kendall test modified by effective sample size to detect trend in serially correlated hydrological series. *Water resources management,* 18(3), 201-218. https://doi.org/10.1023/B:WARM.0000043140.61082.60

Zarazúa Villaseñor, P., Ruiz Corral, J. A., Ramírez Ojeda, G., Medina García, G., Rodríguez Moreno, V. M., Mora Orozco, C. D. L., ... & Durán Puga, N. (2014). Índices de extremos térmicos en las Llanuras Costeras del Golfo Sur en México. *Revista Mexicana de Ciencias Agrícolas*, 5(SPE10), 1843-1857. http://www.scielo.org.mx/scielo.php?script=sci_arttext&pid=S2007-09342014001401843&lng=es&tlng=es (last accessed: August 2024).

ANNEX A. Table of extreme climate indices for maximum and minimum temperature.

Extreme climate Indices	Time scale	Means	units
csdi5	Annual	Cold spell duration indicator 5-day window **(when the minimum temperature (TN) remains below its climatological 10th percentile)**	Days
csdi	Annual	Cold spell duration indicator **(when the minimum temperature (TN) remains below its climatological 10th percentile)**	Days
dtr	Annual and monthly	Daily Temperature Range	Degrees_C
gddgrow10	Annual	Growing Degree Days	Degree-days
gsl	Annual	Growing Season Length	Days
hddheat18	Annual	Heating Degree Days	Degree-days
hw	Annual	Heatwave	Degrees_C or number of wave
su	Annual and monthly	Summer days	Days
tmge10	Annual and monthly	TX of at least 10 degrees_C	Days
tmge5	Annual and monthly	TX of at least 5 degrees_C	Days
tmm	Annual and monthly	Mean TM	Degrees_C
tn10p	Annual and monthly	Amount of cold nights **(10th percentile)**	%
tn90p	Annual and monthly	Amount of hot days	%
tnm	Annual and monthly	Mean TN	Degrees_C
tnn	Annual and monthly	Min TN	Degrees_C
tnx	Annual and monthly	Max TN	Degrees_C
tr	Annual and monthly	Tropical nights	Days
tx10p	Annual and monthly	Amount of cool days	%
tx3tn3	Annual	3 consecutive number of hot days and nights	Number of events
tx90p	Annual and monthly	Amount of hot days	%
tx95t	Daily	Very warm day threshold	Degrees_C
txb3tnb3	Annual	3 consecutive number of cold days and Nights	Number of events
txge30	Annual and monthly	TX of at least 30 degrees_C	Days
txge35	Annual and monthly	TX of at least 35 degrees_C	Days
txgt50p	Annual and monthly	Fraction of days with above average temperature	%
txm	Annual and monthly	Mean TX	Degrees_C
txn	Annual and monthly	Min TX	Degrees_C
txx	Annual and monthly	Max TX	Degrees_C
wsdi5	Annual	Warm spell duration indicator (5day)	Days
wsdi	Annual	Warm spell duration indicator **(when the maximum temperature (TX) remains above its climatological 90th percentile)**	Days

ANNEX B. This study extreme climate indices graphics.

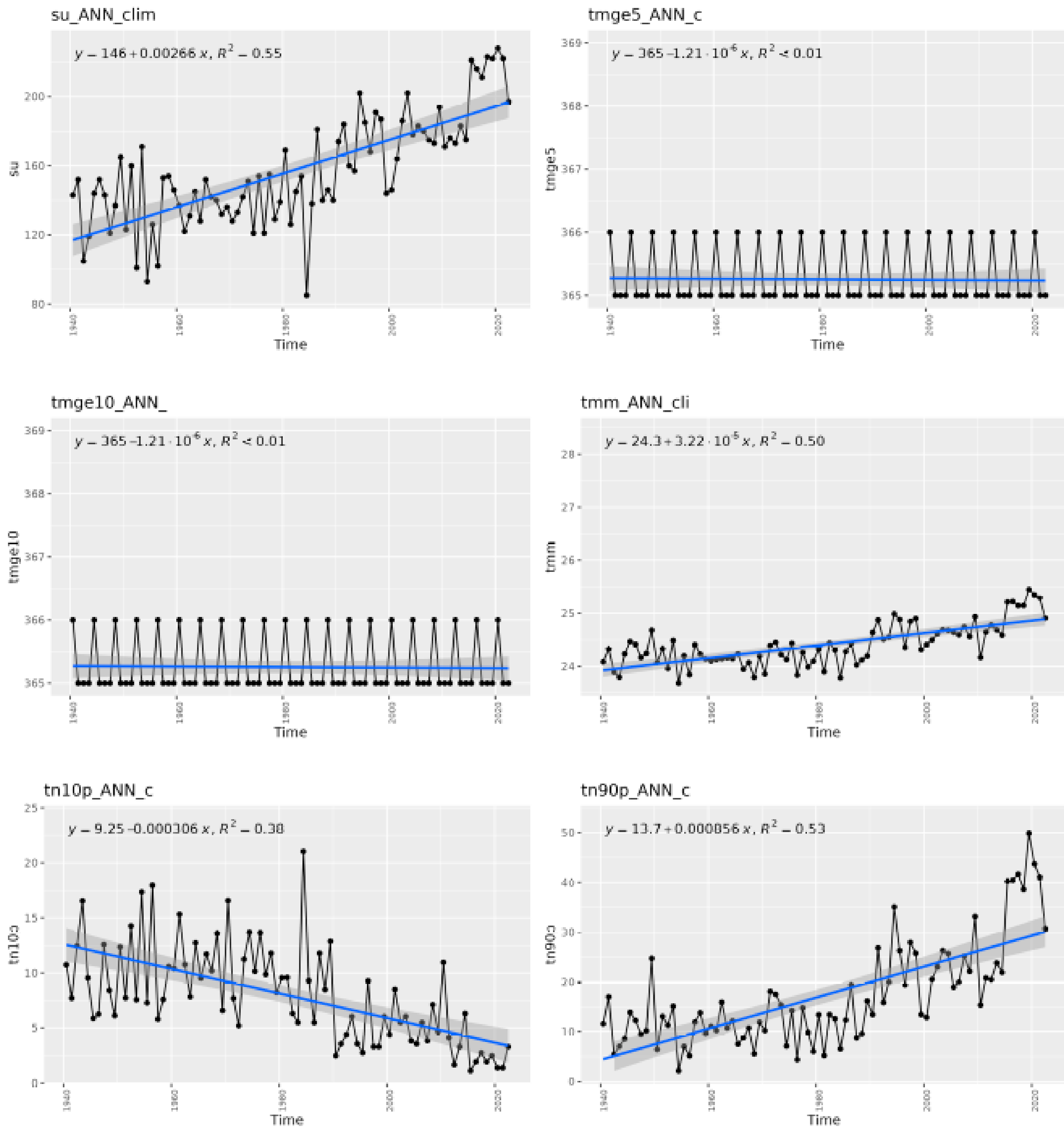

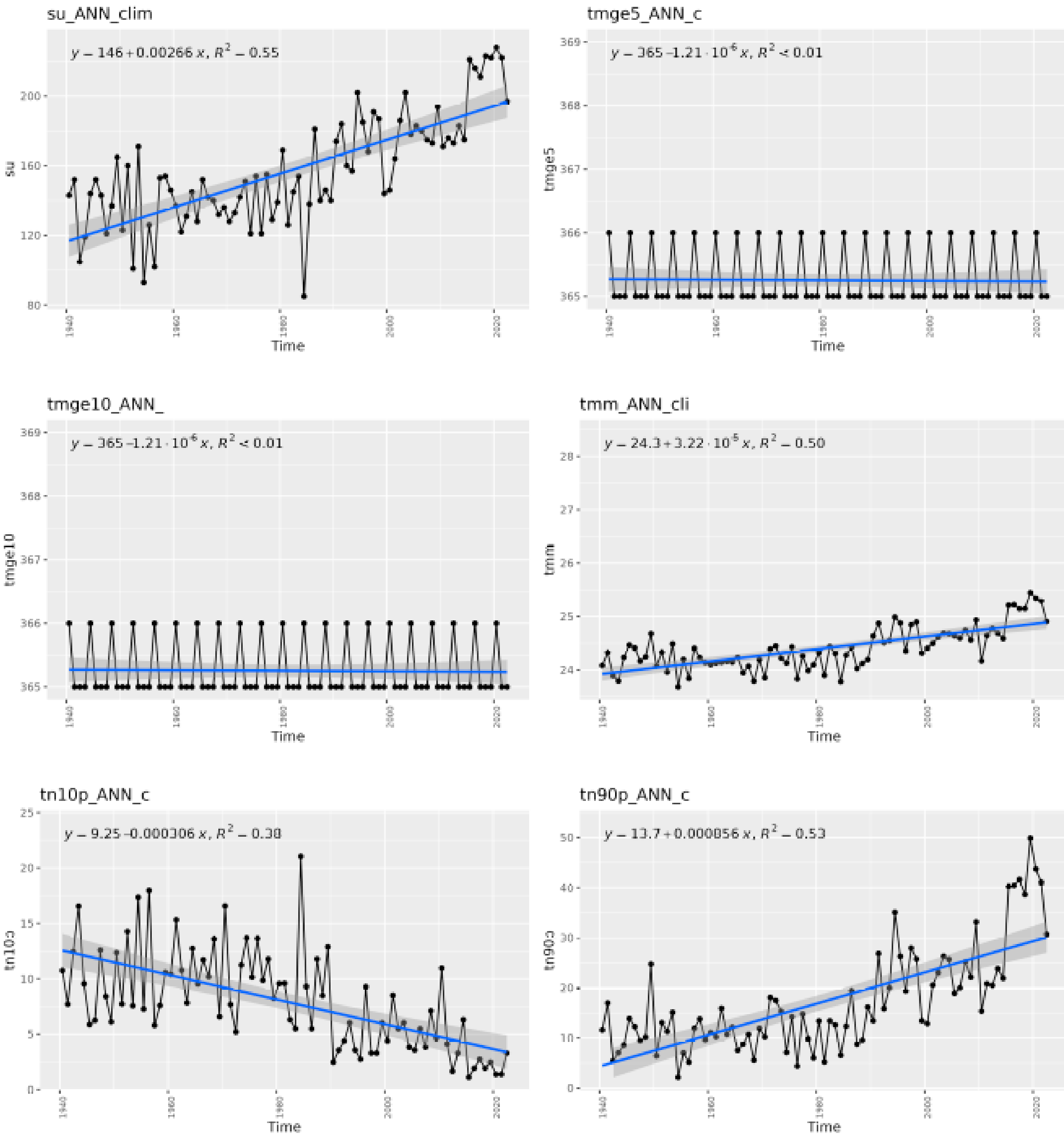
su_ANN_clim
y = 146 + 0.00266 x, R² = 0.55
su
Time
tmge5_ANN_c
y = 365 −1.21 · 10⁻⁶ x, R² < 0.01
tmge5
Time
tmge10_ANN_
y = 365 −1.21 · 10⁻⁶ x, R² < 0.01
tmge10
Time
tmm_ANN_cli
y = 24.3 + 3.22 · 10⁻⁵ x, R² = 0.50
tmm
Time
tn10p_ANN_c
y = 9.25 −0.000306 x, R² = 0.38
tn10p
Time
tn90p_ANN_c
y = 13.7 + 0.000856 x, R² = 0.53
tn90p
Time

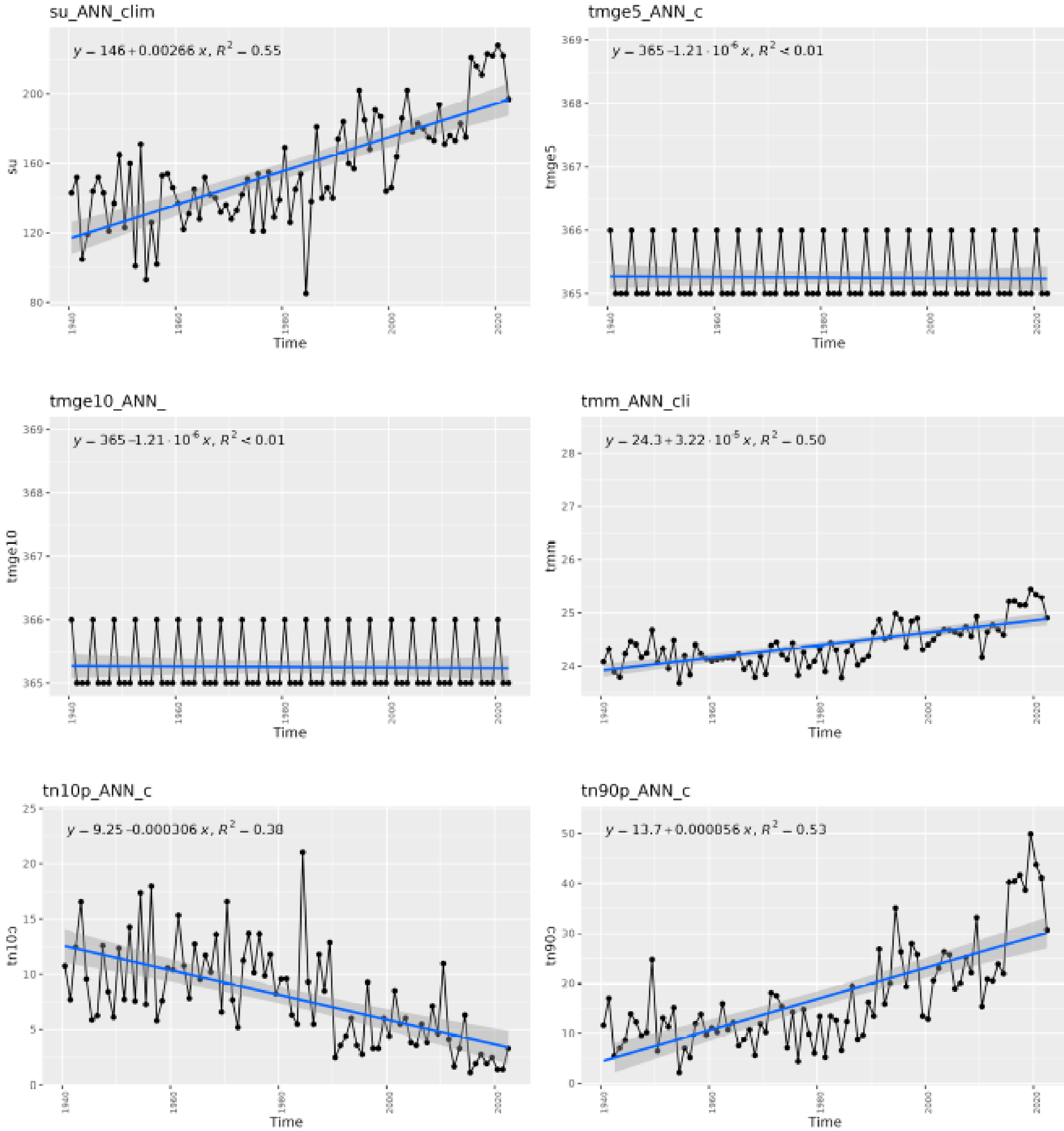
su_ANN_clim
y = 146 + 0.00266 x, R² = 0.55
su
Time
tmge5_ANN_c
y = 365 −1.21 · 10⁻⁶ x, R² < 0.01
tmge5
Time
tmge10_ANN_
y = 365 −1.21 · 10⁻⁶ x, R² < 0.01
tmge10
Time
tmm_ANN_cli
y = 24.3 + 3.22 · 10⁻⁵ x, R² = 0.50
tmm
Time
tn10p_ANN_c
y = 9.25 −0.000306 x, R² = 0.38
tn10p
Time
tn90p_ANN_c
y = 13.7 + 0.000856 x, R² = 0.53
tn90p
Time

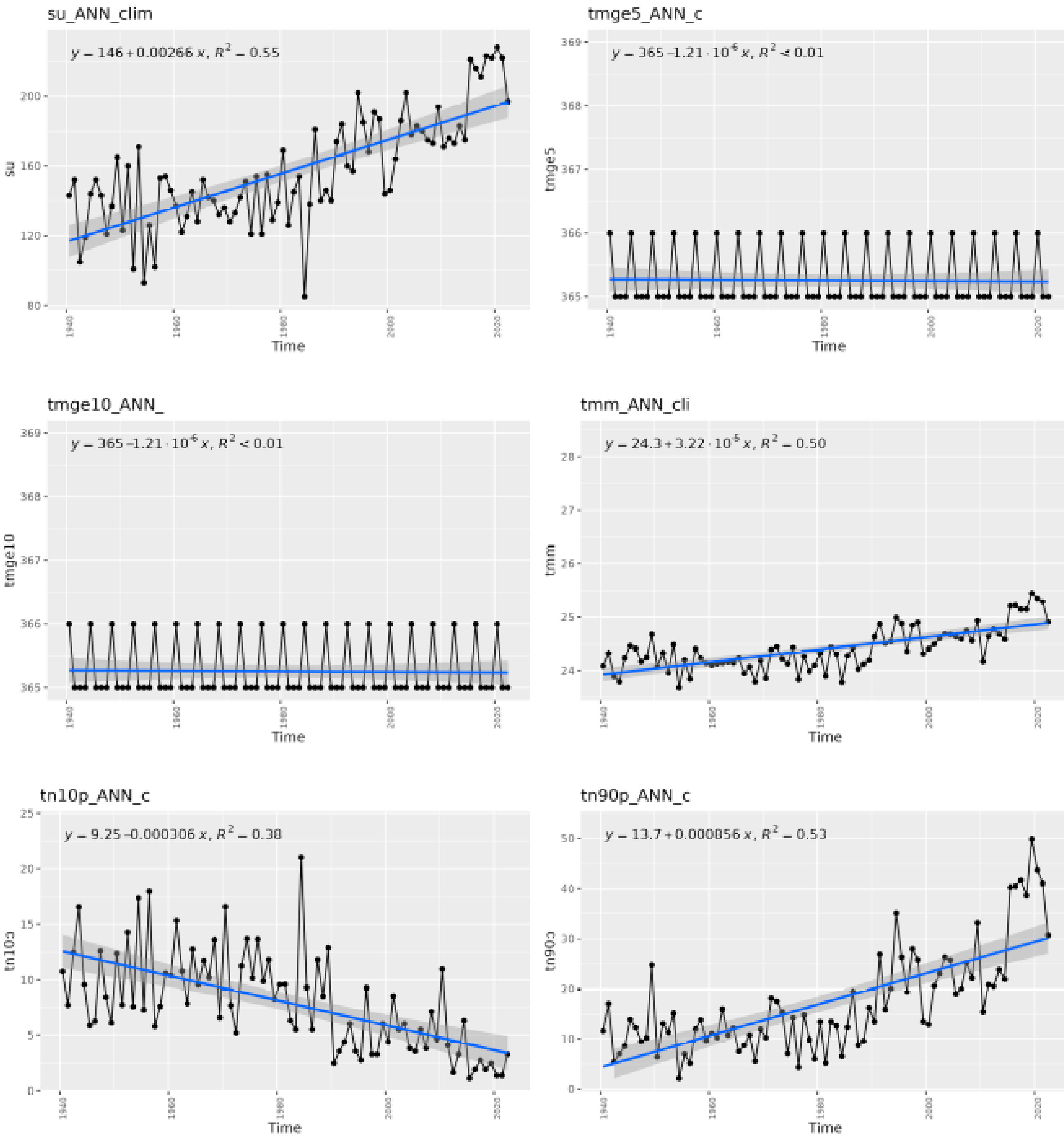
su_ANN_clim
y = 146 + 0.00266 x, R² = 0.55
su
Time
tmge5_ANN_c
y = 365 −1.21 · 10⁻⁶ x, R² < 0.01
tmge5
Time
tmge10_ANN_
y = 365 −1.21 · 10⁻⁶ x, R² < 0.01
tmge10
Time
tmm_ANN_cli
y = 24.3 + 3.22 · 10⁻⁵ x, R² = 0.50
tmm
Time
tn10p_ANN_c
y = 9.25 −0.000306 x, R² = 0.38
tn10p
Time
tn90p_ANN_c
y = 13.7 + 0.000856 x, R² = 0.53
tn90p
Time

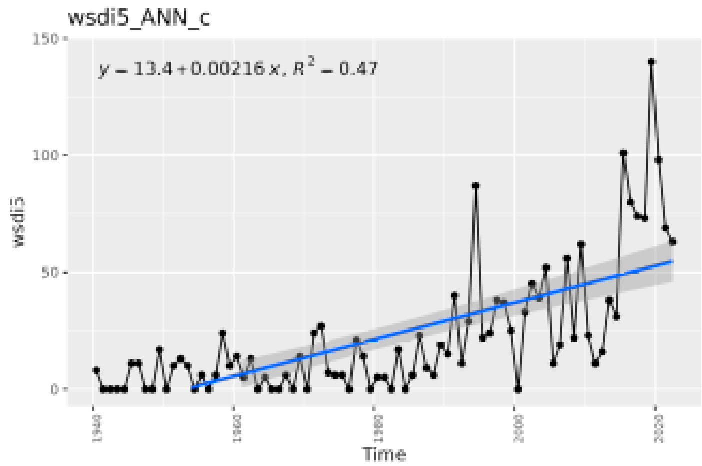
wsdi5_ANN_c
y = 13.4 + 0.00216 x, R^2 = 0.47
wsdi5
150
100
50
0
1940
1960
1980
2000
2020
Time

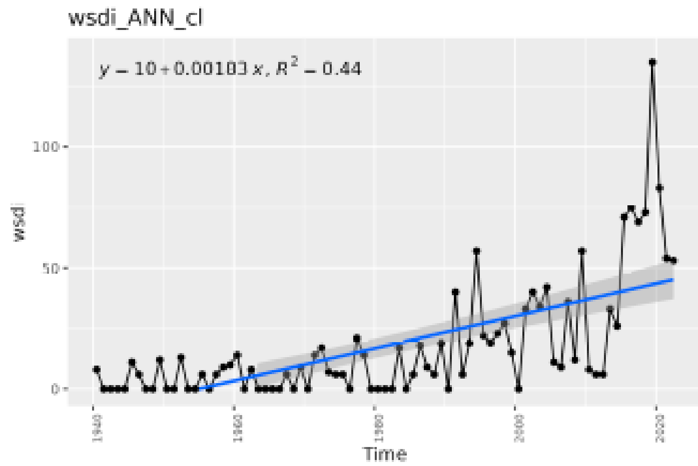
wsdi_ANN_cl
y = 10 + 0.00103 x, R^2 = 0.44
wsdi
100
50
0
1940
1960
1980
2000
2020
Time